

Identifying high redshift AGNs using X-ray hardness

J. X. Wang^{1,3}, S. Malhotra², J. E. Rhoads², C. A. Norman^{1,2}

ABSTRACT

The X-ray color (hardness ratio) of optically undetected X-ray sources can be used to distinguish obscured active galactic nuclei (AGNs) at low and intermediate redshift from viable high-redshift (i.e., $z > 5$) AGN candidates. This will help determine the space density, ionizing photon production, and X-ray background contribution of the earliest detectable AGNs. High redshift AGNs should appear soft in X-rays, with hardness ratio $HR \sim -0.5$, even if there is strong absorption by a hydrogen column density N_H up to 10^{23} cm^{-2} , simply because the absorption redshifts out of the soft X-ray band in the observed frame. Here the X-ray hardness ratio is defined as $HR = (H-S)/(H+S)$, where S and H are the soft and hard band net counts detected by *Chandra*. High redshift AGNs that are Compton thick ($N_H \gtrsim 10^{24} \text{ cm}^{-2}$) could have $HR \sim 0.0$ at $z > 5$. However, these should be rare in deep Chandra images, since they have to be $\gtrsim 10$ times brighter intrinsically, which implies $\gtrsim 100$ times drop in their space density. Applying the hardness criterion ($HR < 0.0$) can filter out about 50% of the candidate high redshift AGNs selected from deep Chandra images.

Subject headings: galaxies: active — galaxies: high-redshift — X-rays: galaxies

1. Introduction

In the past few years, many deep *Chandra* images of the extragalactic sky have been obtained, with the 2 Ms *Chandra* Deep Field North (CDF-N, e.g., Alexander et al. 2003) and 1Ms *Chandra* Deep Field South (CDF-S, Giacconi et al. 2002; Rosati et al. 2002)

¹Department of Physics and Astronomy, Johns Hopkins University, 3400 N. Charles Street, Baltimore, MD 21218; jxw@pha.jhu.edu, norman@stsci.edu.

²Space Telescope Science Institute, 3700 San Martin Drive, Baltimore, MD 21218; san@stsci.edu, rhoads@stsci.edu.

³Center for Astrophysics, University of Science and Technology of China, Hefei, Anhui 230026, P. R. China; jxw@ustc.edu.cn.

being the two deepest. Combining such exposures with deep optical images allows easy selection of candidate high redshift (i.e., $z > 5$, hereafter high- z) AGNs. Such high- z AGNs are extremely faint in optical bands blueward of the $\text{Ly}\alpha$ wavelength, because of the heavy absorption of UV light by the high redshift IGM (e.g., Fan et al. 2001). Optically undetected X-ray sources are thus good candidates for high-redshift AGNs. Their space density provides an upper limit on the density of high- z AGNs, and can help determine their cosmological evolution and contribution to reionization (e.g., see Alexander et al. 2001; Barger et al. 2003a; Koekemoer et al. 2004; Wang et al. 2004). However, the absence of these candidates in optical bands makes them difficult to identify spectroscopically. This motivates different approaches to studying them. Currently, the efforts mainly focus on their infrared colors (e.g., Yan et al. 2003; Koekemoer et al. 2004).

In this letter, we point out for the first time that the X-ray hardness ratio can be used to filter out low- z sources from these X-ray selected, optically undetected high- z candidates. High- z AGNs cannot be hard in *Chandra* images, because the absorption that makes the X-ray spectra harder is redshifted out of the soft X-ray band in the observed frame. In section 2, we present detailed simulations to quantify this effect. Here the hardness ratio (HR) is defined as $(\text{H}-\text{S})/(\text{H}+\text{S})$, where S and H are the soft (0.5 – 2.0 keV) and hard (2.0 – 8.0 keV)¹ X-ray band net counts detected by *Chandra*.

2. Simulations

The X-ray spectra of low and intermediate redshift AGNs have been well studied using the observations from several generations of X-ray satellites, including EINSTEIN, ROSAT, ASCA, BeppoSAX, *Chandra*, and XMM. For type 1 AGNs (i.e., Seyfert 1 galaxies, and QSOs), the basic component of their X-ray spectra is a power law with photon index $\Gamma \sim 1.9$ (e.g., Nandra et al. 1997; George et al. 2000, Malizia et al. 2003) and an exponential cut off at high energies (~ 200 keV, see Malizia et al. 2003). For type 2 AGNs (i.e., Seyfert 2 galaxies, and type 2 QSOs), the power law is cut off at low energies by photo-electric absorption, and the cutoff energy increases with the column density of the intercepted torus (e.g., Turner et al. 1997a; Norman et al. 2002). Recent *Chandra* observations show that the X-ray spectra of QSOs (i.e., luminous AGNs) at $z = 4.0 - 6.3$ are also well fitted by a

¹In some papers, only the 2.0 – 7.0 keV band net counts were given (e.g., Giacconi et al. 2002; Stern et al. 2002; Wang et al. 2004). The difference of the hardness ratios (HR) using different hard bands (2.0 – 8.0 keV or 2.0 – 7.0 keV) is negligible ($\Delta\text{HR} < 0.008$ from our simulations). This is actually expected because *Chandra* has much lower effective area above 7 keV and 7.0 – 8.0 keV X-ray net count makes a very small contribution to the whole hard band.

power law with photon index $\Gamma = 1.9$ (Vignali et al. 2004). This indicates that although the space density of AGNs varies significantly from $z \sim 0 - 6$, the shape of their intrinsic X-ray spectra evolves relatively little. Evidence for warm absorbers and/or soft excess emission (e.g., Krolik & Kriss 2001; Piro, Matt & Ricci 1997) have also been found in significant numbers of AGNs. However, at high- z , these features shift out of *Chandra*’s soft band.

In this section we present simulations to predict the X-ray colors in *Chandra* images for high- z AGNs by assuming a power law spectrum ($\Gamma = 1.9$) with different absorption column densities ($N_H = 10^{21}, 10^{22}, 10^{23}, 10^{24} \text{ cm}^{-2}$ respectively; see Fig. 1 for the model spectra). We used XSPEC 11.0.1 to do the simulations, and model *wabs* in XSPEC, a photoelectric absorption using Wisconsin cross-sections (Morrison and McCammon, 1983), to simulate the neutral absorption in the rest frame. The *Chandra* ACIS on-axis instrument response for CDF-S (Giacconi et al. 2002) was used, and the Galactic HI column density ($N_H = 0.8 \times 10^{20} \text{ cm}^{-2}$) in CDF-S was taken account during the simulations². The output X-ray hardness ratios are plotted in Fig. 2. We can see that the predicted HR is a constant (-0.58 for $\Gamma = 1.9$) for AGNs without intrinsic absorption at any redshift, because of the power law shape of the X-ray spectrum. The corresponding HR for different photon indices are also shown in Fig. 2. While the photon index for QSOs varies from 1.5 to 3.0 (e.g., George et al. 2000), the dominant source of variation in hardness ratio HR is absorption. We show in Fig. 2 that an extreme power-law with $\Gamma = 1.5$ would still give a soft color ($\text{HR} = -0.41$). For AGNs with intrinsic absorption, the predicted hardness ratio varies with redshift: at lower redshift, the X-ray spectra are much harder because the soft X-ray emission are significantly attenuated by the absorber; but at $z > 5$, we barely see differences between the X-ray hardness ratios of X-ray spectra with absorption up to $N_H = 10^{23} \text{ cm}^{-2}$, because the absorption has largely redshifted out of the soft X-ray band. If the absorber is Compton thick ($N_H \geq 10^{24} \text{ cm}^{-2}$), even the hard X-ray emission would be significantly attenuated. At $z > 5$, the predicted hardness ratio is ~ 0.0 . In the compton thick regime ($N_H = 10^{24} \text{ cm}^{-2}$), further correction to photoelectric absorption is needed, due to Compton scattering (see Matt, Pompilio & La Franca 1999; Yaqoob 1997). Based on figure 3 of Matt et al. (1999) which includes compton scattering, we conclude that the *shape* of the transmitted curve is unchanged by compton scattering, while the amplitude decreases by a factor of 1.7.

For higher column density ($N_H > 10^{24} \text{ cm}^{-2}$), the direct X-ray emission is strongly attenuated, and the X-ray spectra are dominated by a reflection component from cold and neutral gas (e.g., Turner et al. 1997b). We used the XSPEC model *pexrav* (Magdziarz &

²Using slightly different Galactic HI column density, or *Chandra* on-axis instrument response calculated for other ACIS-I fields, does not affect any results presented in this paper.

Zdziarski 1995) to simulate such pure reflection spectra.³ The Fe K emission line at 6.4 keV has a higher equivalent width (EW) in the reflection dominated X-ray spectra of AGNs (e.g., Ghisellini, Haardt & Matt 1994; Levenson et al. 2002) since the direct component is absent. Therefore we add an Fe K emission line at 6.4 keV with EW of 1 keV in the rest frame, which is normal in the reflection dominated X-ray spectra of AGNs (e.g., Levenson et al. 2002).

3. Discussion

The X-ray spectra of AGNs at low to intermediate redshifts can be extremely hard due to heavy absorption (with hardness ratios up to $HR \sim 1.0$). However, they are much softer at higher redshift because the absorbed energy shifts out of the observed bands (see Fig. 2 for simulations, and Fig. 12 of Szokoly et al. 2004 for the HR distribution of a large sample of AGNs from $z = 0-4$). AGNs at $z \gtrsim 5$ with intrinsic absorption up to $N_H = 10^{23} \text{ cm}^{-2}$ should have $HR \sim -0.5$, and the Compton-thick ones ($N_H \gtrsim 10^{24} \text{ cm}^{-2}$) should have $HR \lesssim 0.1$. Due to heavy absorption, and Compton scattering, the X-ray flux of Compton-thick AGNs ($N_H \sim 10^{24} \text{ cm}^{-2}$) is attenuated by a factor of 9.5 (See Fig. 1).

For pure reflection spectra, the attenuation is even larger: assuming a reflection efficiency of 3% in rest frame 2.0 – 10.0 keV band (e.g., see Norman et al. 2002) yields a factor of 21. Thus any high redshift sources detected with a large hardness ratio would have intrinsic X-ray luminosity of $\sim 10^{45} \text{ erg s}^{-1}$. We know that brighter QSOs are much rarer; according to the X-ray luminosity function of AGNs (e.g., see Miyaji, Hasinger, & Schmidt 2001; Ueda et al. 2003), a tenfold increase in luminosity implies a hundredfold drop in the space density. Furthermore, there is evidence that the fraction of type 2 AGNs decreases at higher intrinsic luminosity (e.g., Steffen et al. 2003; Ueda et al. 2003). We conclude that those candidates with $HR \gtrsim 0.0$ are statistically unlikely to be at $z \gtrsim 5$. They are either obscured AGNs or QSOs at low to intermediate redshift.

Chandra has detected a number of AGNs at high redshift. Presently, there are 66 AGNs⁴ at $z > 4$ detected by *Chandra* ACIS, and 41 of them have published soft (0.5 – 2.0

³The model of Magdziarz & Zdziarski is angle-dependent. The results we present in this paper were derived by setting $\cos\theta$ at 0.45, which is closest in overall shape to the reflected spectrum averaged over all viewing angles. Reflection from smaller viewing angles tends to be slightly harder ($\Delta HR < 0.1$), but obviously, this is not the case for type II AGNs which are supposed to edge-on.

⁴See the excellent Web site <http://www.astro.psu.edu/users/niel/papers/highz-xray-detected.dat> maintained by Niel Brandt and Christian Vignali for the list of the high-redshift AGN detected in X-rays so far

keV) and hard (2.0 – 8.0 keV) band net counts (or 0.5 – 2.0 keV band and 0.5 – 8.0 keV band net counts) (Alexander et al. 2003; Barger et al. 2002; Brandt et al. 2001, 2002; Castander et al. 2003; Vignali et al. 2001, 2003a, 2003b; Bassett et al. 2004). All of the 41 sources have $HR \leq 0.0$, with an average value of -0.60 ± 0.21 , in excellent agreement with our estimates above. All of these sources are type 1 AGNs, and most of them are optically selected. Since strong X-ray emission is expected from both type 1 and type 2 AGNs, we expect the X-ray selected high- z AGN sample to include both types. However we argue that the hardness ratio distribution of the X-ray selected high- z AGNs should be similar to that of the known $z > 4$ AGNs based on following reasons: I) the 3 X-ray selected AGNs with $z > 4$ have consistent soft X-ray colors with the rest; II) high- z type 2 AGNs with N_H upto 10^{23} cm^{-2} are also expected to be X-ray soft with $HR \sim -0.5$; III) type 2 AGNs with heavier absorption are much fainter in observed X-ray fluxes, thus are much rarer.

Wang et al. (2004) presented 168 X-ray sources detected by an 172 ks *Chandra* ACIS exposure in the Large Area Lyman Alpha (LALA, e.g, Rhoads et al. 2003) Boötes field. 19 of them are not detected in deep R and bluer band images ($R > 25.7$, Vega mag) and are possible $z \gtrsim 5$ objects. The sources and their hardness ratios are listed in Table 1 of Wang et al. In Fig. 3, we plot their hardness ratios comparing with the 41 *Chandra* detected $z > 4$ AGNs. The two distributions are distinguishable at 99.99% level according to the Kolmogorov-Smirnov (K-S) test. Down to a flux limit of $1.7 \times 10^{-15} \text{ ergs cm}^{-2} \text{ s}^{-1}$, the 19 sources contribute $\sim 8\%$ to the total 2 – 10 keV band X-ray background (Wang et al. 2004). After removing sources with $HR > 0$, we lose 50% of the candidates and the contribution to the total X-ray background drops to $\sim 4\%$.

Yan et al. (2003) studied the infrared colors of 6 R band nondetected X-ray sources in CDF-S. These sources are listed in table 1. Two of them have $HR \gtrsim 0.0$, and cannot be at $z > 5$. This agrees with Yan’s statement, that all these sources are unlikely to be at $z > 5$ based on their infrared colors. Koekemoer et al. (2004) presented 7 X-ray sources in CDF-S which are undetected in deep multi-band GOODS HST ACS images, with extremely high X-ray-to-optical ratios and red colors ($z_{850} - K$). These sources might be located at $z > 6$ such that even their $\text{Ly}\alpha$ emission is redshifted out of the bandpass of ACS z_{850} filter. We find that 3 of the 7 sources have $HR \gtrsim 0.0$, indicating that their X-ray colors are too hard to be at $z > 6$. These 3 sources could instead be type 2 AGNs at low to intermediate redshift. Their nuclear optical emission should be heavily obscured, and their host galaxies need to be substantially underluminous, or dust-obscured, compared to other known sources (Koekemoer et al. 2004). This confirms that there is a population of AGNs at low to intermediate redshift which are extremely red, with high X-ray-to-optical ratios, and undetected at the depth of GOODS. The analogous sample among non-active galaxies is the population of extremely red objects (EROs), which have surface density comparable to

Lyman break galaxies but a much lower typical redshift (e.g., Vaisanen & Johansson 2004).

Using deep multicolor optical data, Barger et al. (2003a) searched candidate $z > 5$ AGNs in the 2 Ms X-ray exposure of the CDF-N, and found that besides the one X-ray source spectroscopically confirmed at $z = 5.19$, only 31 X-ray sources with $z' > 25.2$ and no B or V band detection could lie at $z > 5$. Barger et al. (2003b) provided multiband photometry for the CDF-N X-ray sources, which allows us to identify the 31 candidate high- z AGNs⁵. The hardness ratio distribution of the 31 sources is plotted in Fig. 3. 15 of the 31 sources have hardness ratios $HR > 0.0$, and thus cannot have $z > 5$. This directly supports the deduction that the majority of the optically undetected X-ray sources are extreme examples of the optically faint X-ray source population, most of which are obscured AGNs at $z \leq 3$ (Alexander et al. 2001). Barger et al. (2003a) pointed out that Haiman & Loeb (1999) overestimated the surface density of $z > 5$ AGNs by at least an order of magnitude, and similar conclusions can be seen in Alexander et al. (2001) and Szokoly et al. (2004). Our analyses indicate that applying the X-ray hardness ratio cutoff ($HR > 0.0$) could further reduce the surface density of candidate $z > 5$ AGNs, and strengthen the above conclusions by a factor of 2. This also supports the statement that AGNs made little contribution to the reionization at $z \sim 6$ (Barger et al. 2003a; also see Dijkstra, Haiman & Loeb 2004; Moustakas & Immler 2004).

4. Conclusions

In this letter we present detailed simulations showing that high- z AGNs cannot be hard in *Chandra* images since X-ray absorption will shift out of soft band at high redshift. High redshift AGNs should appear soft in X-rays, with hardness ratio $HR \sim -0.5$ at $z \gtrsim 5$, even if there is strong absorption with N_H up to 10^{23}cm^{-2} . High- z AGNs that are Compton thick ($N_H \gtrsim 10^{24} \text{cm}^{-2}$) could have $HR \sim 0.0$. However, these should be rare in deep Chandra images, since they have to be $\gtrsim 10$ times brighter intrinsically, which implies $\gtrsim 100$ times drop in their space density. Most optically undetected X-ray sources with $HR \gtrsim 0.0$ should be obscured AGNs at low to intermediate redshift. Applying the hardness criterion ($HR < 0.0$) can filter out about 50% of the candidate high redshift AGNs selected from deep Chandra

⁵Because the magnitudes discussed in Barger et al. 2003a and 2003b were measured with different aperture diameters, it is difficult to pick up exactly the same 31 sources discussed in Barger et al. 2003a based on the magnitudes provided in Barger et al. 2003b. We identify 31 candidate high- z AGNs in CDF-N following the same manner discussed in Barger et al. 2003a (i.e., z' band faint and B, V band undetected), and tune the threshold magnitudes to match the numbers of sources discussed in Barger et al. 2003a. Thus the sample we picked up could statistically represent that of Barger et al. 2003a

images. This criterion can thereby help us to understand the nature of these *Chandra* X-ray sources, put additional robust constraints to the space density of high- z AGNs, and significantly reduce the expensive telescope time needed to spectroscopically confirm high- z AGN samples based on deep *Chandra* images.

We would like to thank Dr. A. Hornschemeier and T. Yaqoob for helpful discussions. The work of JW was supported by the CXC grant GO2-3152x and GO3-4148X. We also would like to thank the referee for a prompt and helpful report.

REFERENCES

- Alexander, D. M., et al. 2001, *AJ*, 122, 2156
- Alexander, D. M., et al. 2003, *AJ*, 126, 539
- Barger, A. J., et al. 2002, *AJ*, 124, 1839
- Barger, A. J., et al. 2003a, *ApJ*, 584, L61
- Barger, A. J., et al. 2003b, *AJ*, 126, 632
- Basset, L. C., Brandt, W. N., Schneider, D. P., Vignali, C., Chartas, G., & Garmire, G. P. 2004, *AJ* in press, astro-ph/0404543
- Brandt, W. N., et al. 2001, *ApJ*, 122, 1
- Brandt, W. N., et al. 2002, *ApJ*, 569, L5
- Castander, F. J., et al. 2003, *AJ*, 125, 1689
- Dijkstra, M., Haiman, Z., & Loeb, A. 2004, *ApJ* submitted, astro-ph0403078
- Fan, X. et al. 2001, *AJ*, 121, 54
- Ghisellini, G., Haardt, F., & Matt, G., 1994, *MNRAS*, 267, 743
- Giacconi, R., et al. 2002, *ApJS*, 139, 369
- George, I. M., et al. 2000, *ApJ*, 531, 52
- Haiman, Z., & Loeb, A. 1999, *ApJ*, 512, L9
- Koekemoer, A. M., et al. 2004, *ApJ*, 600, L123
- Krolik, J. H., & Kriss, G. A. 2001, *ApJ*, 561, 684
- Levenson, N. A., Krolik, J. H., Życki, P. T., Heckman, T. M., Weaver, K. A., & Awaki, H. 2002, *ApJ*, 573, L81

- Lyons, L. 1991, *Data Analysis for Physical Science Students*, Cambridge University Press, Cambridge
- Magdziarz, P., & Zdziarski, A. 1995, *MNRAS*, 273, 837
- Malizia, A., Bassani, L., Stephen, J. B., & Di Cocco, G. 2003, *ApJ*, 589, L17
- Matt, G., Pompilio, F., La Franca, F. 1999, *NewA*, 4, 191
- Miyaji, T., Hasinger, G, & Schmidt, M. 2001, *A&A*, 369, 49
- Morrison, R., & McCammon, D. 1983, *ApJ*, 270, 119
- Moustakas, L. A. & Immler, S. 2004, *ApJL* submitted, astro-ph0405270
- Nandra, K., George, I. M., Mushotzky, R. F., Turner, T. J., & Yaqoob, T. 1997, *ApJ*, 477, 602
- Norman, C. et al. 2002, *ApJ*, 571, 218
- Piro, L., Matt, G., & Ricci, R. 1997, *A&AS*, 126, 525
- Rhoads, J. E. et al. 2003, *AJ*, 125, 1006
- Rosati, P., et al. 2002, *ApJ*, 566, 667
- Steffen, A. T., Barger, A. J., Cowie, L. L., Mushotzky, R. F., & Yang, Y. 2003, *ApJ*, 596, L23
- Stern, D., et al. 2002, *AJ*, 123, 2223
- Szokoly, G. P. et al. 2004, *ApJS* submitted, astro-ph0312324
- Turner, T. J., George, I. M., Nandra, K., Mushotzky, R. F. 1997a, *ApJS*, 113, 23
- Turner, T. J., George, I. M., Nandra, K., Mushotzky, R. F. 1997b, *ApJ*, 488, 164
- Ueda, Y., Akiyama, M., Ohta, K., & Miyaji, T. 2003, *ApJ*, 598, 886
- Vaisanen, P., & Johansson, P. H. 2004, *A&A*, 421, 821
- Vignali, C., et al. 2001, *AJ*, 122, 2143
- Vignali, C., Brandt, W. N., & Schneider, D. P. 2004, in *ASP Conf. Series, AGN Physics with the SDSS*, eds. G.T. Richards and P.B. Hall, astro-ph0310659
- Vignali, C., Brandt, W. N., Schneider, D. P., Garmire, G. P., Kaspi, S. 2003a, *AJ*, 125, 418
- Vignali, C., et al. 2003b, *AJ*, 125, 2876
- Wang, J. X., et al. 2004, *AJ*, 127, 213
- Yan, H, et al. 2003, *ApJ*, 585, 67

Yaqoob, T. 1997, ApJ, 479, 184

Table 1. CDF-S X-ray sources in Koekemoer et al. 2004 and Yan et al. 2003

ID ^a	R.A(J2000)	Dec.(J2000)	HR ^b
Koekemoer et al. 2004			
66	3:32:08.39	-27:40:47.0	0.30 ^{+0.17} _{-0.17}
69 ^c	3:32:08.89	-27:44:24.3	-0.71 ^{+0.52} _{-0.29}
93	3:32:13.92	-27:50:00.7	-0.32 ^{+0.11} _{-0.68}
133	3:32:20.36	-27:42:28.5	-0.01 ^{+0.28} _{-0.30}
161	3:32:25.83	-27:51:20.3	-0.29 ^{+0.21} _{-0.71}
191	3:32:33.14	-27:52:05.9	-0.35 ^{+0.11} _{-0.65}
216	3:32:51.64	-27:52:12.8	0.15 ^{+0.22} _{-0.23}
Yan et al. 2003			
98 ^d	3:32:14.67	-27:44:03.4	0.09
140	3:32:22.44	-27:45:43.9	-0.39 ^{+0.25} _{-0.61}
188	3:32:32.17	-27:46:51.4	0.39 ^{+0.15} _{-0.16}
214	3:32:38.03	-27:46:26.2	-0.45 ^{+0.08} _{-0.08}
222	3:32:39.06	-27:44:39.1	-0.11 ^{+0.10} _{-0.10}

^aX-ray Source ID in Giacconi et al. (2002).

^bThe X-ray net counts in different bands used to calculate HR are from Alexander et al. (2003). We subtract the soft band net counts from the total band (0.5 – 8.0 keV) net counts to calculate the hard band net counts for sources with only upper limits of the hard band net counts in Alexander et al. Errors for this quantity are calculated following the "numerical method" described in §1.7.3 of Lyons 1991.

^cAlso included by Yan et al. 2003.

^dOnly 0.5 – 8.0 keV band net count is available in Alexander et al., and the hardness ratio is derived using the upper limit of the soft and hard band counts, the sum of which is very close to the total count (32.2 vs 27.9).

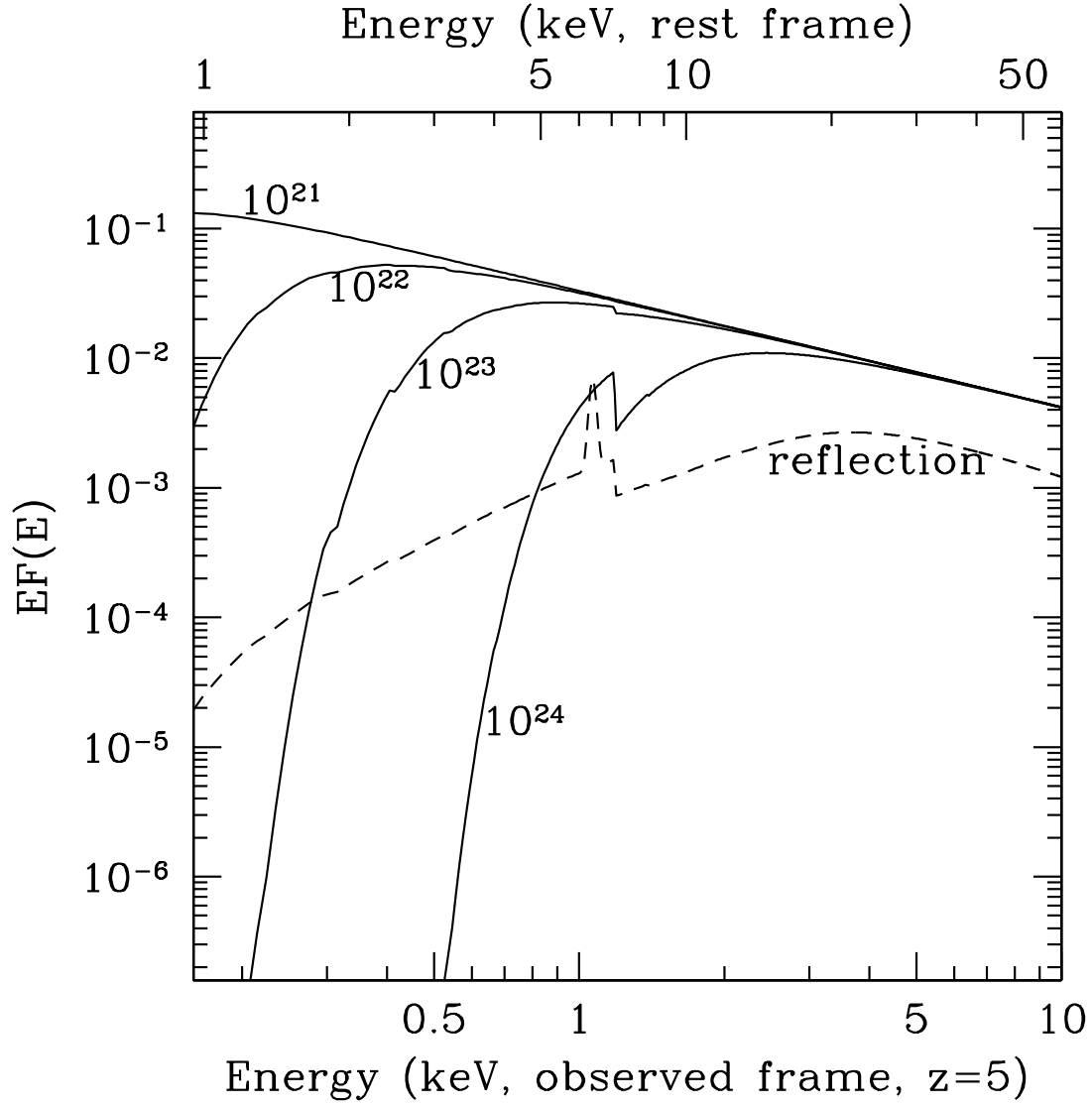


Fig. 1.— The input model spectra for $N_H = 10^{21}, 10^{22}, 10^{23}, 10^{24} \text{ cm}^{-2}$, and pure reflection spectrum.

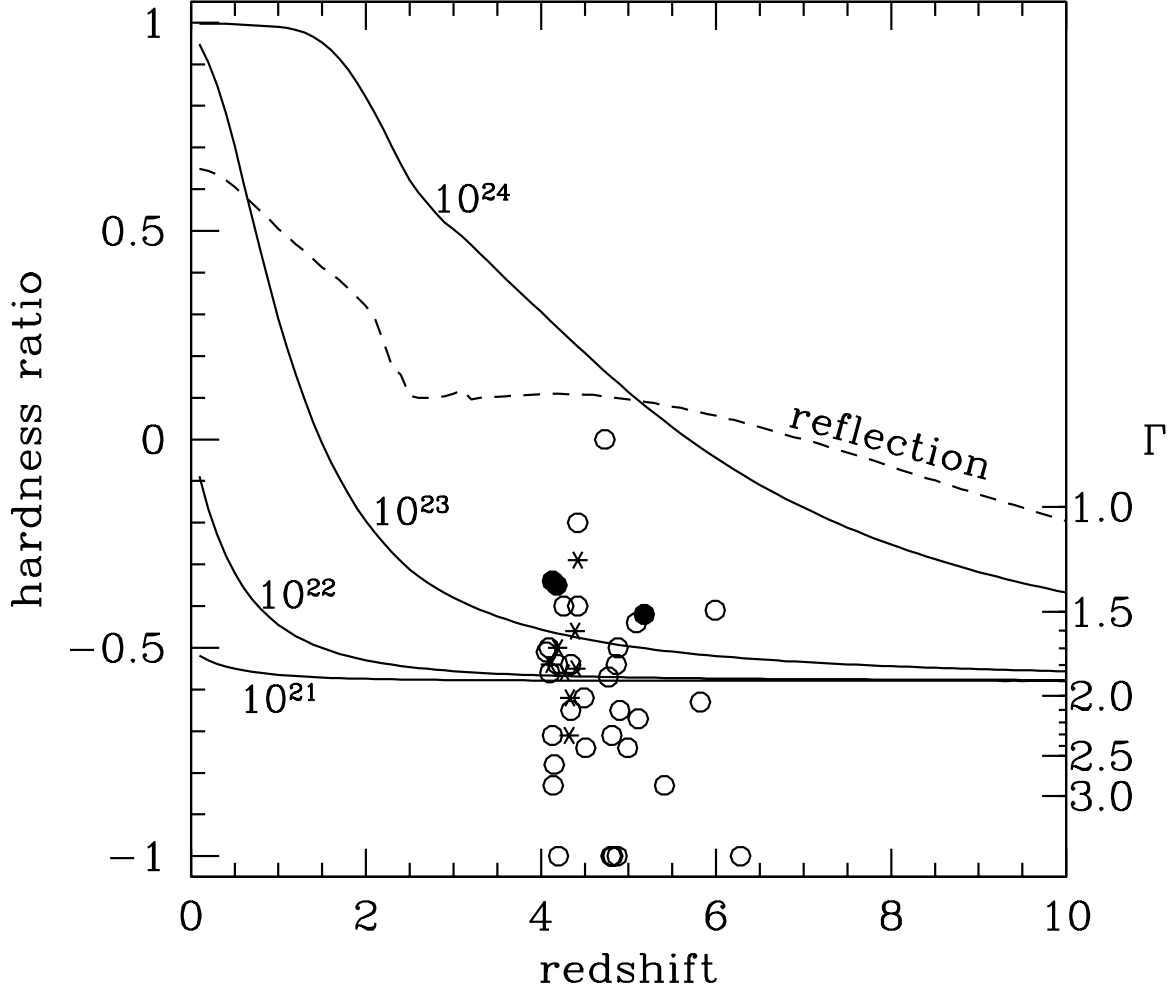


Fig. 2.— The predicted X-ray hardness ratio HR at different redshift. The input spectrum is a power law with photon index $\Gamma = 1.9$, and absorbed by different column densities in the rest frame ($N_H = 10^{21}$, 10^{22} , 10^{23} , and 10^{24} cm $^{-2}$ respectively) and pure reflection spectrum. The output is the hardness ratio, if observed by *Chandra*. The hardness ratio HR is defined as $(H-S)/(H+S)$, where H and S are *Chandra* net counts in the soft (0.5 – 2.0 keV) and hard (2.0 – 8.0 keV) X-ray band. Along the right ordinate, we mark the photon indices Γ of absorption-free power-law spectra which could reproduce the corresponding hardness ratios. The known AGNs at $z > 4$ detected by *Chandra* are also marked: open circles are optically selected, solid circles are X-ray selected, and stars are radio selected. See Fig. 12 of Szokoly et al. 2004 for a sample of *Chandra* detected AGN at $z < 4$.

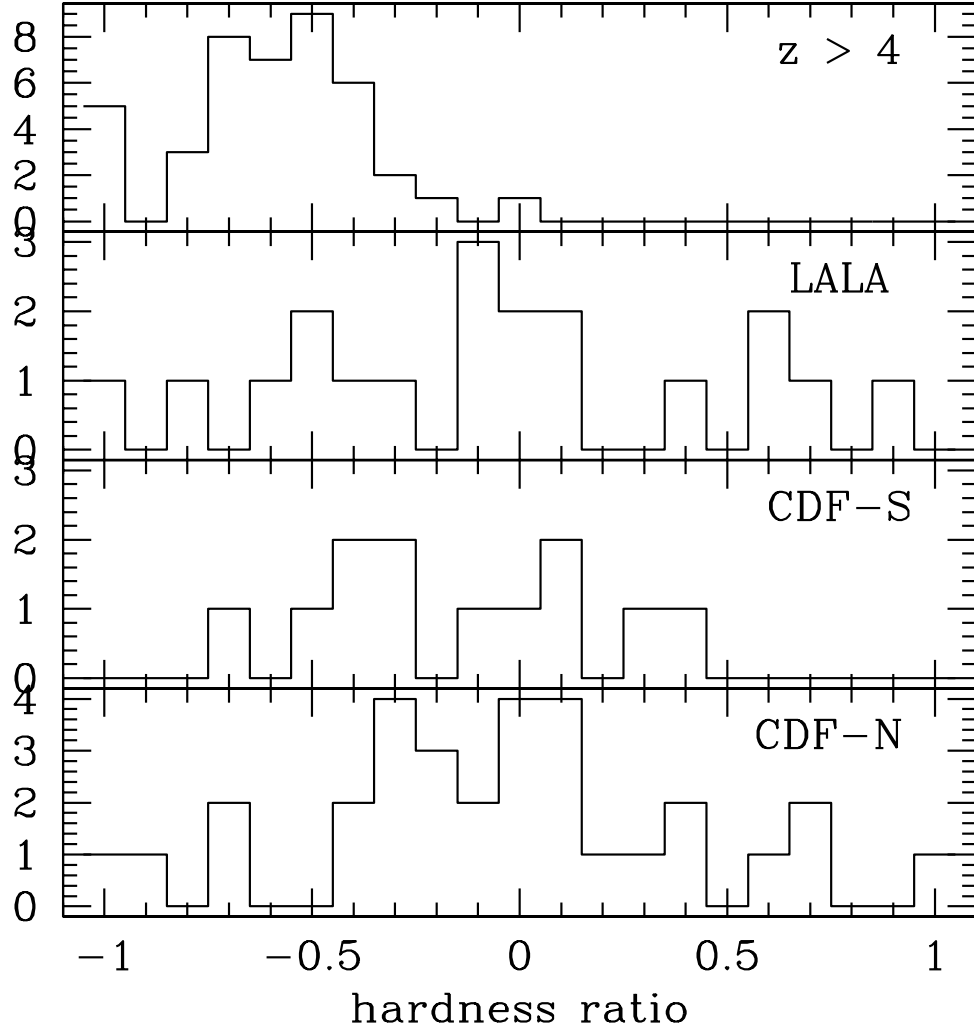


Fig. 3.— The X-ray hardness ratio distributions of 41 *Chandra* detected $z > 4$ AGNs ($z > 4$), 19 high- z candidates in LALA Boötes field (LALA), 12 CDF-S sources in Koekemoer et al. (2004) and Yan et al (2003), and 31 CDF-N sources discussed in Barger et al. (2003a). The later three distributions are significantly different from the first one at the level $> 99.99\%$ based on the K-S test. See the text for details.